

Fig. S1. Patterning of the organ of Corti and β -catenin expression in the cochlear duct. (A) Transverse section through an E14.5 cochlear duct immunolabeled with β -catenin antibody (red) and an antibody against the prosensory marker Sox2 (green). The asterisk indicates the presumptive organ of Corti (OC) domain; β -catenin labeling is shown in white at right. (B) High-magnification luminal surface view of the midbase of a P1 OC. Expression of β -catenin (red, left) is observed in the cell membranes. The HCs are labeled for myosin 6 (Myo6, green, middle); the row of inner HCs (IHC) is indicated, and the rows of outer HCs are numbered (1-3). The support cell nuclei are labeled for Sox2 (white, right); the two rows of pillar cells (PCs) and three rows of Deiter's cells (DCs) are indicated. (C) Confocal digitally created z-stack transverse section through a P0 OC; all antibodies are shown merged at top and singly below; β -catenin (red, second row), Myo6 (green, third row) and DAPI (blue, bottom row). GER, greater epithelial ridge; LER, lesser epithelial ridge.

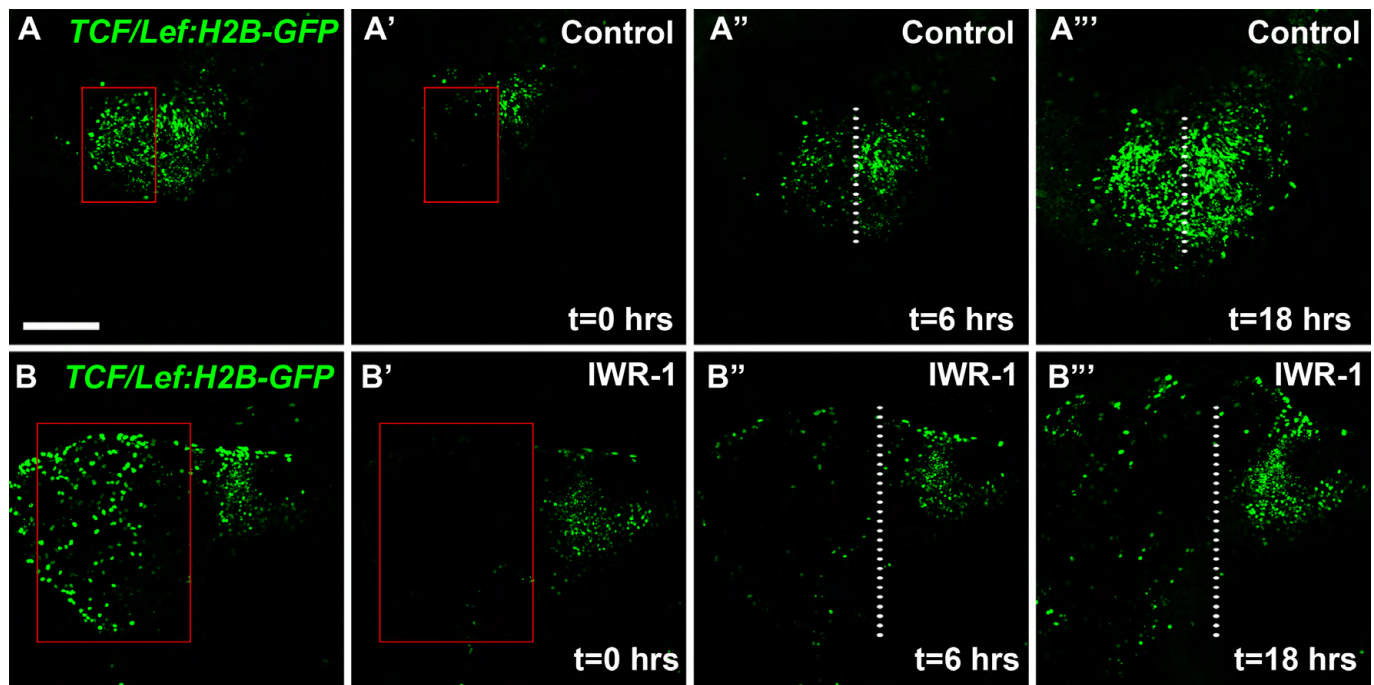


Fig. S2. Inhibition of canonical Wnt signaling blocks GFP reporter activity. (A,B) Low-magnification images of E13.5 cochlear explants transfected with the *TCF/Lef:H2B-GFP* reporter construct shown after 48 hours in vitro. A defined region (red box) from each explant was photobleached using a Zeiss LSM 510 confocal laser microscope by running the 488 laser at 100% power with 300 passes at a pixel scan speed of 6.4 μ s. (A',B') Immediately after photobleaching (referred to as time 0, $t=0$), explants were treated with culture media containing either DMSO as a control (A') or with 150 μ M of the Wnt inhibitor IWR-1 (B'). (A'',B'') Explants shown 6 hours after photobleaching/application of drug ($t=6$ hrs). At this point, many cells in control explants have recovered high levels of GFP reporter activity within the photobleached region (A''), whereas the Wnt inhibitor-treated explants show minimal fluorescence recovery (B''). (A''',B''') Similarly, 18 hours after photobleaching/treatment ($t=18$ hrs), control samples show almost full recovery of GFP reporter activity within the photobleached region (A'''). By contrast, most cells in the photobleached region of Wnt inhibitor-treated samples fail to recover (B'''), demonstrating the specificity of both the reporter and the inhibitor. Scale bar: 200 μ m.

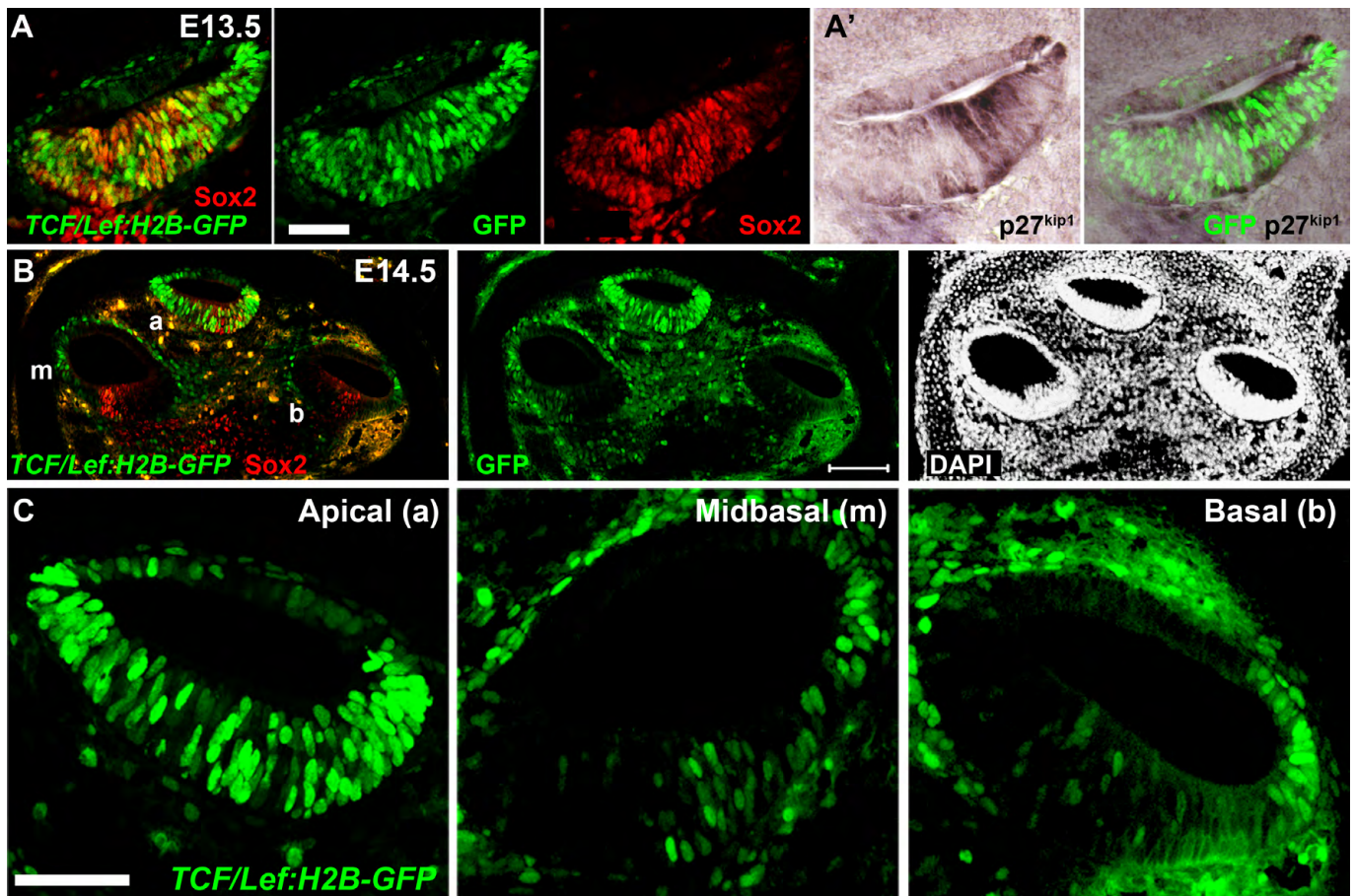


Fig. S3. Cross-sections through E13.5 and E14.5 *TCF/Lef:H2B-GFP* reporter mouse cochleae. (A,A') Alternate transverse sections through the apical turn of an E13.5 *TCF/Lef:H2B-GFP* reporter mouse cochlea showing fluorescent immunohistochemistry for the GFP reporter and Sox2 expression (A) and alkaline phosphatase (DAB) immunohistochemistry for p27^{kip1} (A') in the early prosensory domain. GFP and p27^{kip1} expression in the alternate sections are shown merged in the far right panel. (B) Low-magnification transverse section of the E14.5 cochlea shown in Fig. 1. GFP (green) and Sox2 (red) are shown merged at left, GFP alone in the middle panel, and DAPI alone far right. (C) High-magnification views of the apical (a), midbasal (m) and basal (b) regions from the above section showing just GFP reporter expression, in which activity is high in the apical region and decreases toward the basal end. Note that the midbasal section has been flipped in the horizontal plane so that in all three high-magnification views medial is to the left and lateral is to the right. Scale bars: 50 μ m in A,C; 100 μ m in B.

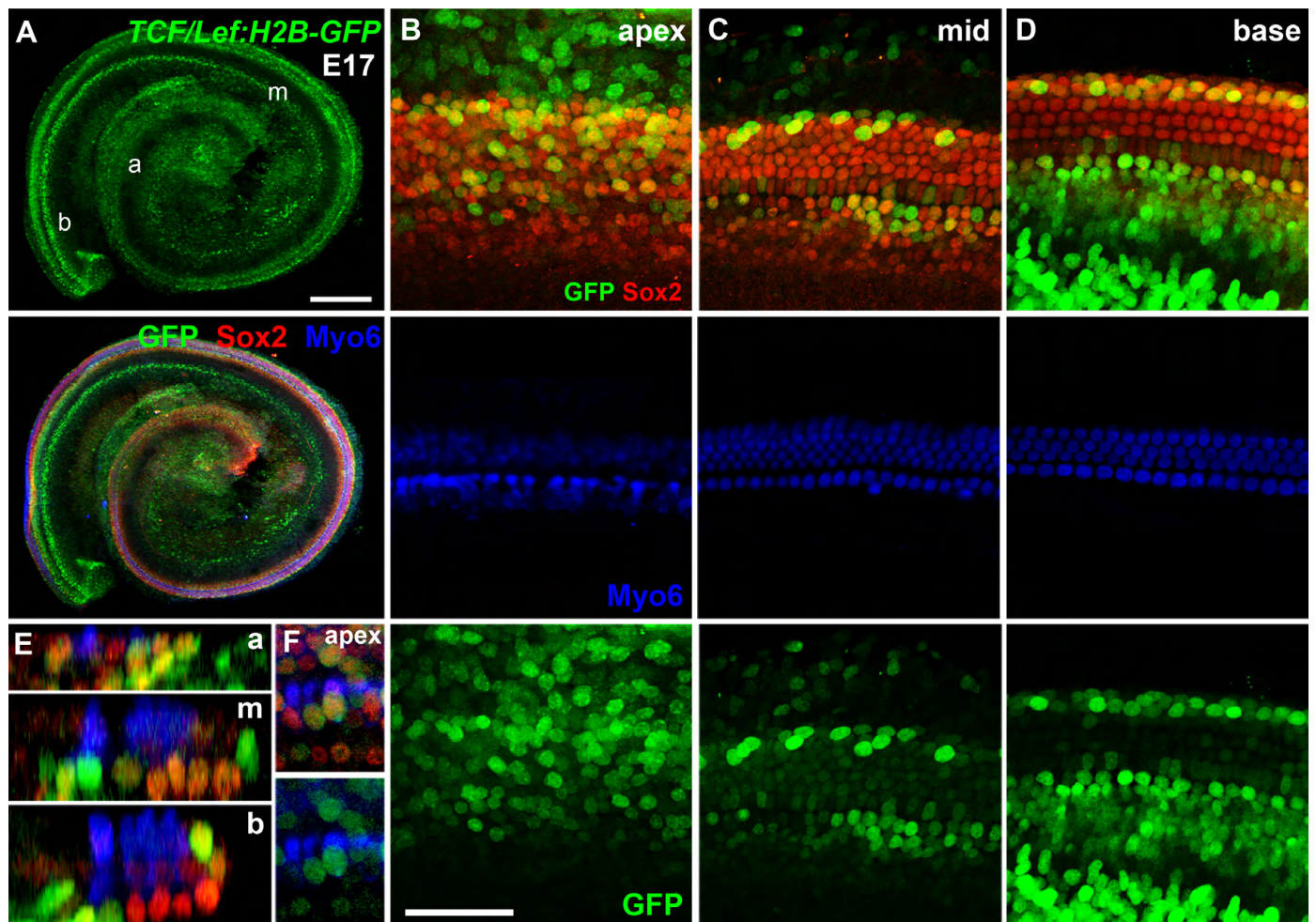


Fig. S4. In vivo canonical Wnt/ β -catenin reporter activity in the E17.5 sensory epithelium. (A-D) Low- (A) and high- (B-D) magnification surface views of the cochlear sensory epithelium from an E17.5 *TCF/Lef:H2B-GFP* reporter mouse immunostained for GFP (green), Sox2 (red) and myosin 6 (Myo6, blue) expression. The apical (a), mid (m) and basal (b) regions are indicated in A. High magnifications of the basal (B), mid (C) and apical (D) regions are shown; Sox2 and GFP are shown in the top panels, Myo6 in middle panels, and GFP alone in the bottom panels. (E) High-magnification confocal z-stack transverse sections through the basal (top) mid (middle) and apical (bottom) regions showing the changing distribution of GFP throughout the OC. (F) High-magnification surface views of GFP-positive apical inner HCs; all three channels shown at top, Myo6 and GFP shown at bottom. Note that in the imaging of E17.5 cochleae, the settings were calibrated to the brightest apical regions in these samples; thus, although signals appear very intense compared with the E14.5 mid and basal regions (see Fig. 1 and Fig. S3), the actual levels of GFP luminescence are more equivalent to the basal region in the E14.5 samples. Scale bars: 250 μ m in A; 50 μ m in B-D.

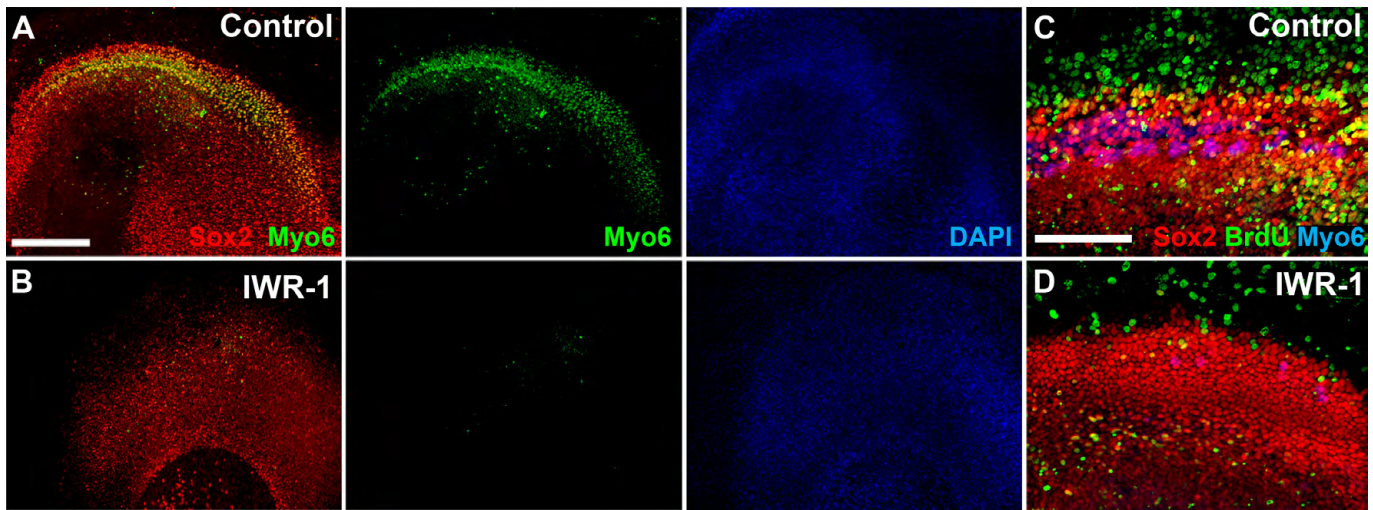


Fig. S5. The Wnt inhibitor IWR-1 blocks HC formation and proliferation in the developing cochlear duct. (A,B) Low-magnification luminal surface views of E12 explants maintained for 5 DIV in either control media (A) or 150 μM of the Wnt inhibitor IWR-1 (B). Similar to the effects of FH535, treatment of E12 explants with the Wnt inhibitor IWR-1 blocks HC differentiation (HCs labeled with Myo6, green) and proliferation and also reduces Sox2 expression (red). Sox2 and Myo6 shown merged in top panel, Myo6 shown alone in middle panel and DAPI-labeled nuclei (blue) are shown in the bottom panel. **(C,D)** Higher-magnification images of the mid-basal region from E12.75 cochlear explants maintained in control media (C) or IWR-1 (D) along with BrdU (labeled in green) for 4 DIV. Many BrdU-positive/Sox2-positive (green/red) cells are present in control explants (C), while very few are observed in IWR-1-treated explants (D). Control explants also have numerous differentiated HCs (C; labeled with Myo6 in blue), while almost no HCs form in IWR-1-treated explants (D). Scale bar: A and B, 200 μm; C and D, 100 μm.

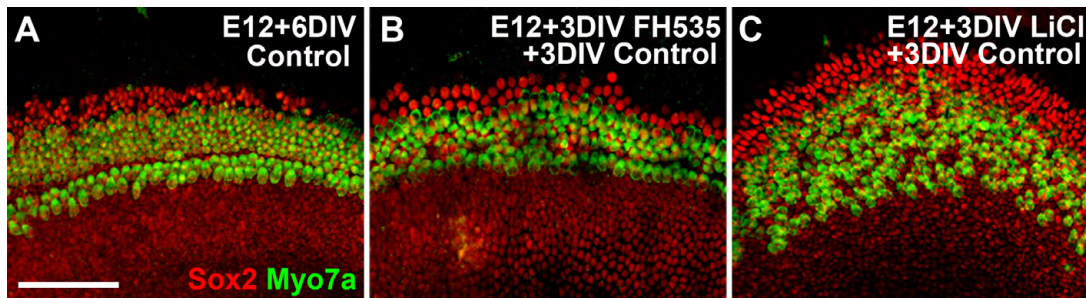


Fig. S6. Transient exposure of E12 explants to the Wnt modulators FH535 or LiCl. Luminal surface views of cochlear sensory epithelial cultures established at E12 and maintained for 6 DIV in control media (A) or transiently exposed to the canonical Wnt inhibitor FH535 (B) or the canonical Wnt activator LiCl (C) for 3 DIV, after which point treated explants were washed in control media then maintained for an additional 3 DIV under control conditions ($n=6$ explants analyzed per condition). The boundary of the OC is indicated by the expression of Sox2 (red) and the HCs are indicated by immunolabeling for myosin 7a (green). Unlike 6-day FH535 treatment, which causes a significant reduction in HC formation (see Fig. 3), a relatively normal pattern of HCs differentiate if FH535 is removed from the medium (B). Conversely, transient LiCl exposure results in an increase in the number of HCs compared with control (C), similar to that observed following a 6-day treatment with LiCl (see Fig. 3). Scale bar: 100 μm .

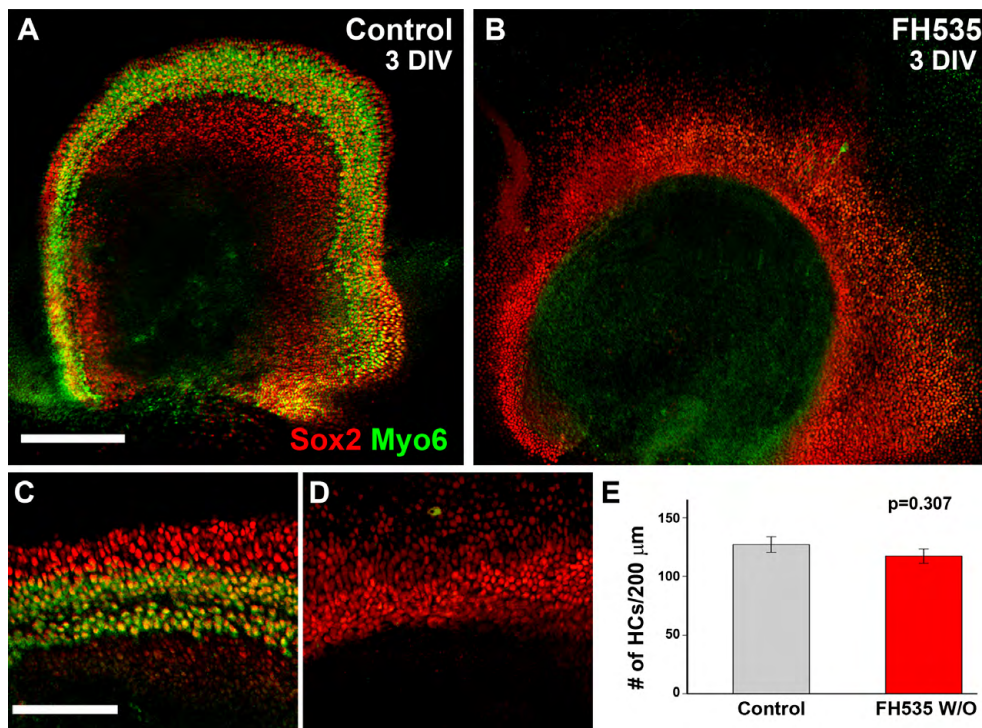


Fig. S7. Loss of HC differentiation induced by FH535 treatment is reversible. (A-D) Low- and high-magnification luminal surface views of E13.5 explants (whole explants shown in A and B, midbasal regions shown in C and D) maintained for 3 DIV in either control media (A,C) or media containing the canonical Wnt inhibitor FH535 (B,D) and immunostained for Sox2 (red) and Myo6 (green). After 3 DIV, no HCs are present in the FH535-treated explant, whereas control explants have an almost mature complement of HCs. (E) Quantification of the number of HCs (counted as the number of HCs per 200 μm at the basal-apical midpoint) that form in control explants and explants transiently exposed to FH535 (cultures were established at E13.5, maintained in FH535 for 3 DIV, followed by an additional 3 DIV in control media; see Fig. 6 for images of these explants after a total of 6 DIV). There was no significant difference between the number of HCs in control and transiently exposed FH535 cultures ($P=0.307$; $n=7$ control and $n=6$ FH535 explants counted) demonstrating that removal of FH535 from the medium enables HC differentiation to begin, and after another 3 DIV a relatively normal complement of HCs forms. Error bars represent s.e.m. Scale bars: 200 μm in A,B; 100 μm in C,D.

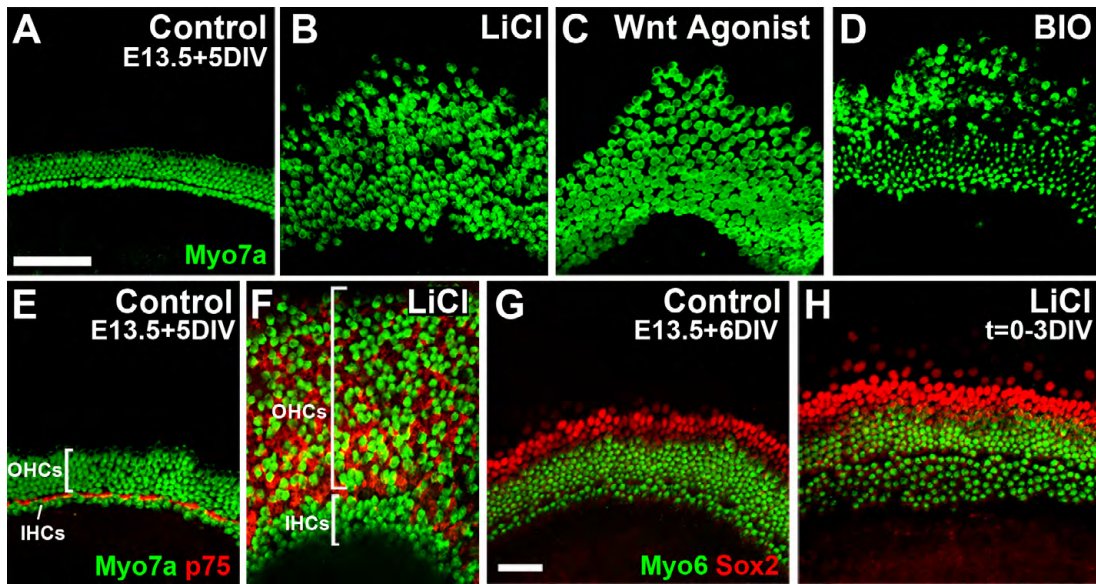


Fig. S8. Wnt/ β -catenin pathway activation induces supernumerary inner and outer HC and supporting cell formation. (A-D) High-magnification images of the luminal surface of E13.5 explants maintained for 5 DIV in either 10 mM NaCl medium (control, A) or canonical Wnt activators: 10 mM LiCl (B), a Gsk3 β inhibitor; 0.75 μ M Wnt Agonist (C), a direct activator of the TCF/Lef level of the pathway (Liu et al., 2005); or 3 μ M BIO (D), another inhibitor of Gsk3 β (Meijer et al., 2003). HCs are labeled for myosin 7a (Myo7a, green). Wnt-activated explants show a significant increase in the number of differentiated HCs (B-D) compared with controls (A). (E,F) Similar view and treatment as above showing control (E) and LiCl-treated (F) explants immunolabeled for Myo7a (green) and p75^{ntr} (red) to indicate the support cells; the inner and outer HC regions are indicated by brackets (IHC and OHC, respectively). (G,H) High-magnification luminal views of Myo6 (green) and Sox2 (red) expression in E13.5 epithelia treated with control media for 6 DIV (G), or with LiCl for 3 DIV followed by incubation for an additional 3 days in control media (H). Following removal of LiCl from the media (H), a relatively normal pattern of Sox2 and Myo6 expression, similar to control (G), is present, although the overall width of the OC is expanded and a significant increase in HCs is observed (H). Scale bars: 100 μ m in A-F; 50 μ m in G,H.

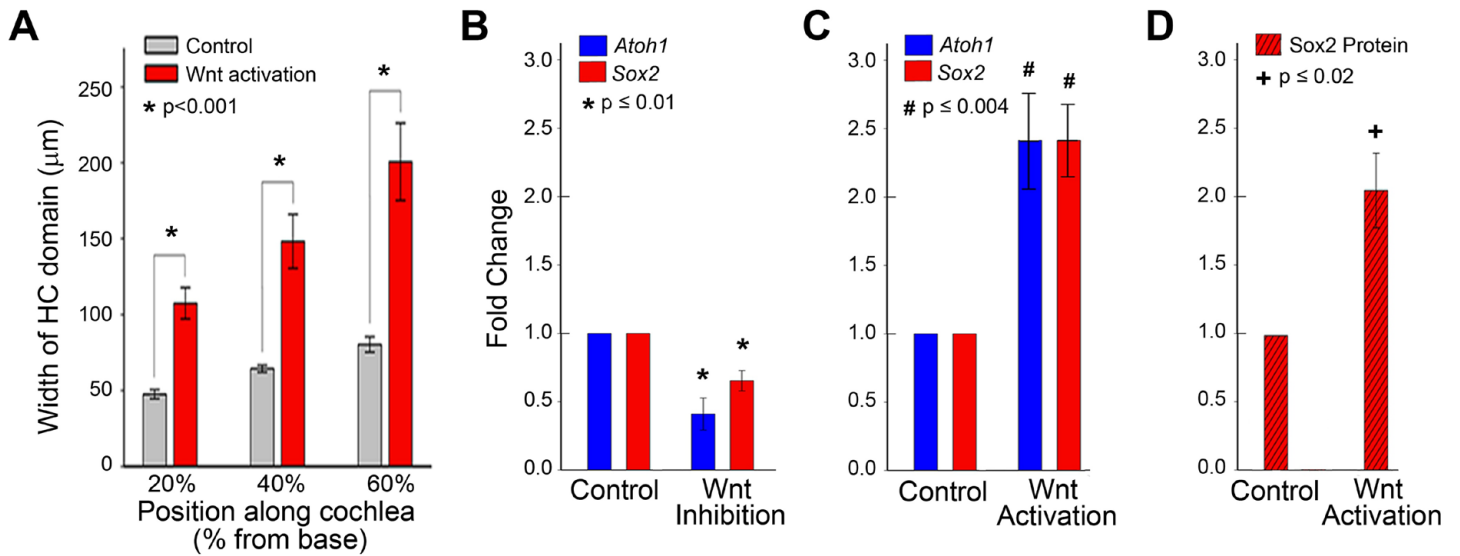


Fig. S9. Quantification of the effects of Wnt/ β -catenin modulation on OC size and expression of Sox2 and Atoh1. (A) The width of the HC domain was measured (from medialmost inner HC to lateralmost outer HC) at the basal-apical midpoint in E13.5 cultures that were exposed to 10 mM LiCl for 3 DIV followed by an additional 3 DIV in control media, as well as in control cultures maintained for 6 DIV ($n=9$ explants per condition). Analysis revealed a significant expansion in the HC domain following LiCl treatment (A). (B,C) Relative qRT-PCR was performed on E13.5 explants maintained for 5 DIV for *Sox2* and *Atoh1* with *Gapdh* as the endogenous control. (B) Wnt inhibition with 3 μ M FH535 significantly reduced both *Sox2* and *Atoh1* ($n=3$ independent qRT-PCR runs performed on three independent sets of explants). (C) Following Wnt Agonist treatment, both *Sox2* and *Atoh1* mRNA levels showed at least a 2-fold increase ($n=5$ independent qRT-PCR runs and sample sets). (D) We also examined the Wnt-mediated induction of Sox2 at the protein level in the same Wnt Agonist and control explants used for mRNA analysis. We utilized an antibody-based qPCR technique based on proximity ligation technology (Fredriksson et al., 2002; Swartzman et al., 2010) that generates results similar to, but more sensitive than, western blotting and enables concurrent analysis of protein and mRNA from the same tissue. Using biotinylated antibodies specific to Sox2 and cathepsin B (as an endogenous loading control), we identified a significant increase in the relative level of Sox2 protein expression compared with control ($n=3$ runs from independent sample sets). Error bars represent s.e.m. (A) $*P \leq 0.001$; (B) $*P \leq 0.01$, (C) $\#P \leq 0.004$; (D) $+P \leq 0.02$. Similar increases in Sox2 protein and mRNA were also detected by qRT-PCR in LiCl-treated cultures (data not shown).